

## **SYNTHESIS AND CHARACTERIZATION OF ZEOLITE Y FROM AKILBENZA CLAY: EFFECT OF CRYSTALLIZATION TIME**

Ernest Kentsa<sup>1</sup>, Horace Manga Ngomo<sup>1</sup>, Charles Fon Abi<sup>2\*</sup>, Julius Sami Ndi<sup>1</sup>, Sary Awad<sup>3</sup>, Divine Dingka, Joseph Ketcha Mbadcam<sup>1</sup>

<sup>1</sup>Physical and Theoretical Chemistry Laboratory, Faculty of Science, University of Yaoundé 1, P.O. Box 812, Yaoundé – Cameroon

<sup>2</sup>Department of Chemistry, Higher Teacher Training College, University of Yaoundé 1, P. O. Box 47 Yaoundé – Cameroon.

<sup>3</sup> GEPEA, UMR 6144, DSEE, IMT-Atlantique, Nantes 44307, France

\*To whom all correspondence should be addressed Charles FON ABI, Tel: +237 77 84 29 80, E-mail: [cf\\_abi@yahoo.fr](mailto:cf_abi@yahoo.fr) , / [cfonabi@jutice.com](mailto:cfonabi@jutice.com), Fax: (237) 222 31 89 99.

---

**ABSTRACT:** *In this work, the synthesis of zeolite Y from Akilbenza clay was studied. The crystallization time of the process was investigated in order to reduce the synthesis duration. Metaclay and dealuminated metaclay (METDEA) were synthesized from Akilbenza clay and then used as sources of aluminium and silicon for zeolite Y synthesis using the hydrothermal method of synthesis. The synthesis parameters used were: ageing time 24 hrs, stirring time 3 hrs, crystallization temperature 110 °C and crystallization time varying from 1 to 4 days. The synthesis was unfolded using a 10 M solution of sodium hydroxide. The crystallisation times were 1, 2, 3 and 4 days. The various products obtained in the course of the synthesis process were analyzed by using XRD, X-ray fluorescence, BET, EDX and ATR-FTIR. XRD pattern of the zeolite obtained match with a standard Y zeolite. It was found to have a specific surface area of 149 m<sup>2</sup>/g, an average pore diameter of 10. 2074 nm, a pore volume of 0.0525 cm<sup>3</sup> and a Si/Al ratio of 2.47. All chemical functions found on the material surface are Si-O-Si, Si-O-Al and located between 455.18 and 1250 cm<sup>-1</sup>. The crystal growth increased with the time of crystallization but a minimum of two days was sufficient for the synthesis. Akilbenza clay can be used for the Y-type zeolites synthesis and the crystallization time impacts on the zeolites' crystallization process.*

**KEYWORD:** Akilbenza clay, metakaolinite, dealuminated metakaolinite, zeolite Y

---

## **INTRODUCTION**

Zeolites are crystalline porous solids. Their crystalline framework is constituted of tetrahedral silicate and aluminate ions which are connected together and then form a channel [1]. Due to this disposition, they possess a high cation mobility, uniform pores, high catalytic activity, high surface area and high thermal stability. For those properties, they are used for ionic exchange, separation, petrochemical refining and various applications in the fine chemical industry. Zeolites are becoming the subject of many interests [2].

Zeolites occur naturally or are obtained by synthesis. Natural zeolites have the following characteristics: rich in impurities, pores with heterogeneous dimensions and a low cation exchange capacity [3]. Zeolites obtained synthetically have the advantage of being of better quality due to their purity, pores' size uniformity, and high thermal stability. They thus open the way to several applications [4]. Alkaline fusion and hydrothermal synthesis are often used as methods for zeolites synthesis. The synthesis of Y-type zeolites uses most the second method because it takes place at low temperature and promotes reactants' high reactivity, a low air pollution, easy solution's control, the formation of metastable phases and single condensed phases [4, 5].

Zeolites are produced from aluminate and silicate salts. According to the method of synthesis, zeolite X, Y, A and ZSM5 type are obtained at the end of the process [6, 7]. Y and ZSM5 zeolites are the most sought because they can either be used as an adsorbent or a catalyst [8]. However, the synthesis of zeolites of type Y from the chemical salts as the source of silica and alumina makes the cost of synthesis high and consequently that of the zeolite material obtained. In order to meet the global demand for this material, which is constantly increasing at around 15-20% per year, natural resources made up of silica and aluminum are used for the synthesis [9, 10]. They are volcanic ashes, industrial wastes which are rich in silica, rice cokes, clay etc. Amongst these natural sources, clay is the most used because it is available and possesses at the same time silica and alumina in their crystalline framework which can be isolated for this synthesis [3, 11].

Synthesis protocols for Y-type zeolite from natural precursors is not standardized since it relies on the environment in which the material is extracted [12]. This is the case for clay materials whose chemical composition and crystalline phases vary according to the geological layer of the soil where they are extracted [13]. Consequently, the parameters of synthesis such as crystallization time, ageing time and crystallization temperature vary in accordance with the natural precursor used [14]. This is the case with crystallization time which was found to be 24 hrs. for Chinese Menglan kaolin [15] and 6 hrs. for Ahoko kaolin [14]. In the same light, the synthesis of the NaY zeolite from Surzlay kaolin resulted in a crystallization time of 28 hrs. [14, 16, 17]. From these previous works of other researchers, it is therefore clear that the conditions of zeolite synthesis are not standard. Moreover, only a few studies can be found in the literature on the hydrothermal processing of natural clay under suitable temperature conditions for the synthesis of zeolites. The objective of this work is to show how the zeolite Y (NaY) can be obtained from a clay collected at Akilbenza, a locality in the eastern region of Cameroon. The effect of crystallization time is studied in this work in order to determine the minimum value.

## **MATERIAL AND METHOD**

### **Material and synthesis mixtures**

The clay material was collected at a depth of 2 m below the ground. It was washed with distilled water to remove impurities like organic matter and other particles. Clay particles with sizes less than 2  $\mu\text{m}$  were obtained using the Stocke's method and sun dried [18]. The dried clay was ground, sieved and stored in an oven at 110 °C for further

experiments and analysis. No other chemical or physical treatment was applied prior to this. The zeolite was synthesized in three steps:

- Thermal activation of the clay in order to get metaclay ;
  - Dealumination of metaclay using sulphuric acid to form a product called METDEA
  - Hydrothermal reaction of metaclay and METDEA at various crystallization times in aqueous alkaline medium.
- ❖ **Thermal activation of the clay**

The synthesis of metakaolin is done in a single step. According to research carried out previously by some authors, metakaolin is obtained at a temperature between 500°C and 900°C. Above this temperature, the kaolin is transformed to mulite which is not favourable for the synthesis of zeolites [19]. For this research a mass of 300 g of clay sample was placed in the oven. The temperature of the oven was gradually increased to 750°C at the rate of 10°C/min. It needed three hours for the metakaolin to be obtained at this temperature. This product was characterized and used as reagent for the zeolite synthesis.

❖ **Dealumination of kaolin**

Dealumination was carried out by mixing 150 g of metakaolin with 250 mL of 10 M sulphuric acid. The mixture was agitated under reflux at a constant temperature of 90°C for 10 hrs. The resulting product was cooled to room temperature and separated from water by sedimentation. The product obtained was washed with distilled water until the sulphate ions were removed. The washing was stopped when the supernatant gave a negative test (absence of a white precipitate) with 0.1M BaCl<sub>2</sub>. The product was finally dried and stored in plastic tubes for various analysis and uses. XRD and X-ray fluorescence analysis were carried out on the product.

❖ **Hydrothermal reaction of metaclay and METDEA for Y zeolite Synthesis**

For the synthesis of the zeolite Y, metakaolin was used as a source of aluminum and the dealuminated metakaolin as a source of silica. The synthesis of type Y zeolite as earlier mentioned takes place in three steps as follows; synthesis of the germination gel (1), synthesis of the growth gel (2) and the synthesis of the product from a mixture of the two gels.

➤ **Synthesis of the Germination Gel**

The germination gel was prepared using 75 mL of 10 M of sodium hydroxide solution. 7.51 g of metakaolin were placed in 20 mL of sodium hydroxide(10 M) solution and the mixture agitated for 1h. This mixture constitutes a solution (1). In another conical flask containing 55 mL of 10 M of sodium hydroxide solution, 15.36g of dealuminated metakaolin was introduced. This second mixture (2) was also agitated for 2 hrs at a temperature of 90 °C. The solution (1) was gently introduced into solution (2) under strong agitation. The third solution obtained was then agitated for 1 hr and then the content of the Pyrex Erlenmeyer flask was then placed in a Teflon tube and allowed to stand for 24 h in order to allow for the formation of chemical bonds (ageing time). The final product obtained in the Teflon tube constitutes the Germination Gel.

➤ **Synthesis of the growth gel**

Here a mass of 13.77 g of metakaolin was introduced in 42.5 mL of 10 M NaOH solution in a Pyrex Erlenmeyer. This mixture (1) was agitated for 1h. The solution rich in silica on the other hand was prepared by placing 28.146 g of dealuminated metakaolin in 100 mL solution of 10 M NaOH. This second mixture (2) was then agitated for 2 hrs. at a temperature of 90°C. Mixture (1) was then gently introduced into mixture (2) under strong agitation for an hour. The third solution obtained is the growth gel.

➤ **Synthesis of the final product from a mixture of the two gels.**

For this synthesis, the germination gel was gently poured in the pyrex conica flask under strong agitation into the growth gel. The resultant mixture was then agitated for 24 hrs at a temperature of 90 °C, then poured into a Teflon tube which was then placed in an oven for crystallization to take place. The temperature and time for crystallization to take place were 100 °C and 4 days respectively. In order to determine the minimum time of crystallization, the preceding process was repeated for crystallization times of 1, 2 and 3 days.

**Characterization technique**  
**kmjljjkl**

- **X-ray Diffraction (XRD)**

X-ray Diffraction analysis was carried out on a powder sample. The XRD patterns were monitored by X-ray diffraction ex-situ using the apparatus Siemens D-5000. It has a Ge crystal primary monochromator which contains Ni-filtered Cu K $\alpha$ 1 radiation,  $\lambda = 1.54056 \text{ \AA}$  with  $\theta/2\theta$  diffraction instrument operating in reflection geometry. The tube of copper is run at 40 mA and 40 kV.

The data was collected at a  $2\theta$  angle in the range 5-60°, with a scanning step of 0.02°. All the materials were crushed using an agate mortar and pestle, ground to powder (< 5  $\mu\text{m}$ ) and mounted on an aluminum plate sample holder of volume of 0.1  $\text{cm}^3$ .

- **Fourier Transform Infrared (FTIR)**

The Fourier Transform Infrared (FTIR) spectra of the clay material was recorded in the range 4000-400  $\text{cm}^{-1}$  using a Mattson Genesis II FTIR spectrometer in transmission mode, used in conjunction with a diamond Attenuated Total Reflectance (ATR) accessory. Powdered samples were sieved to give a particle size < 5  $\mu\text{m}$  and then placed onto the diamond ATR crystal surface for analysis.

- **Scanning Electron Microscope (SEM) and EDX**

The morphology of the clay material was investigated by SEM on a JEOL JSM 7600F, JEOL JSM 5800LV scanning electron microscope equipped with a SDD SAMX energy dispersion spectrometer and JEOL (hybrid of two microscopes), under the following analytical conditions: EHT = 20.00 kV, Signal A = SE1, WD = 4.0 mm. The samples were prepared by spray drying the clay material mounted onto aluminum stubs using

double-sided adhesive carbon discs and sputter coated with gold to reduce static charges and then observed under a scanning electron microscope.

For EDX analysis, the samples were prepared in a similar manner to those of the SEM. However, to avoid errors in the aluminum content, a carbon sample holder was used instead of aluminum stud and the samples were not gold-coated.

- **X-ray fluorescence (XRF)**

The chemical composition was determined with a "SHIMADZU" X-ray fluorescence (XRF) analyzer fitted with an EDX 800 HS X-ray tube, a gas scintillation detector and a PR-10 anode.

- **BET Analyzer (Nitrogen sorption)**

The surface area and the porosity of the clay sample were determined by the sorption of nitrogen gas using AZAP 2000 BET analyzer. For this purpose, a mass of 0.5 g of samples was degassed for 1 day to dehydrate the sample and to remove impurities, followed by nitrogen sorption for 24 h.

## **RESULTS AND DISCUSSIONS**

### **Characterization**

#### **Clay**

From the XRD pattern of the clay (Fig 1), it is found that the material is mainly composed of kaolinite (K), (JCPDS card No 06-0221) as indicated by the peaks at  $2\theta = 12.6, 20.1, 21, 24.9, 35, 36.5, 38.5, 39.6, 46, 50.4, 55$  [20-23]. The peak at  $2\theta = 26.7$  indicates the presence of quartz (Q), (JCPDS card No 5-0490). The low intensity peak //at  $2\theta = 6.86$  indicates the presence of illite (I), and mica (M) (JCPDS card No. 26-0911). Hence, Akilbenza clay is found to be richer in kaolinite which is 1:1 consisting of one tetrahedral sheet and one octahedral sheet.

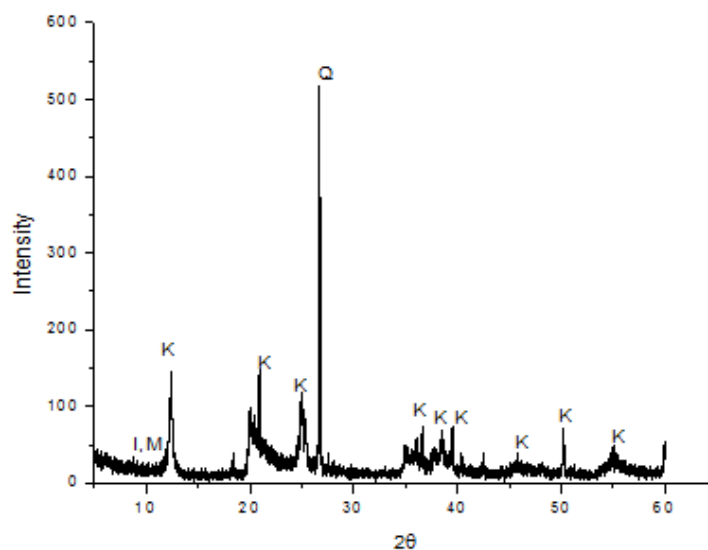


Figure 1: XRD spectra of the Alkibenza clay

From the chemical analysis of the clay by XRF (Table 1), the clay material is mainly composed of silica, aluminum, titanium, iron and potassium. The elements (E), sulfur, phosphorus, calcium, zirconium, chromium, nickel, niobium and zinc are present in trace quantities. The Si/Al ratio 1.41 is higher than the ratio of one for standard kaolinite clay [24]. The excess silicon is as a result of the presence of quartz in this clay material [25].

**Table 1:** Chemical composition (C) of the clay

E	Si	Al	Ti	Fe	K	S	P	Ca	Zr	Cr	Ni	Nb	Zn	Si/Al
C	49.8	35.4	6.0	5.1	1.1	<1	<1	<1	<1	<1	<1	<1	<1	1.41

From the FTIR-ATR spectral (Fig 2), the presence of a large band observed between 3331.16 and 3787.59  $\text{cm}^{-1}$  is characteristic of Al-OH stretching vibration, Al-OH inter octahedral and H-O-H stretching vibrations of kaolinite [26, 27]. The band at 3695  $\text{cm}^{-1}$  corresponds to the stretching vibration modes of OH groups located at the surface of the octahedral sheets opposite to the tetrahedral oxygens adjacent kaolinite layer. Whereas the band at 3623  $\text{cm}^{-1}$  is related to the stretching vibration modes of OH groups which are in the plane common to octahedral and tetrahedral sheets. They are also hydroxyl linkage and water adsorption [28]. The band at 2360.6  $\text{cm}^{-1}$  represents organic materials. Whereas the bands at 1017  $\text{cm}^{-1}$  is attributed to Si-O stretching vibrations while the bands at 1031.09 and 1002.14  $\text{cm}^{-1}$  are as a result of Si-O-Si and Si-O-Al stretching. The band at 907  $\text{cm}^{-1}$  is attributed to OH bending vibration. This band is due to the presence of Al-OH groups [29]. The bands at 776, 689.55, 529.91, 464.57 and 420.7  $\text{cm}^{-1}$  are attributed to Si-O and Al-O vibrations. The presence of Al-O-H at 3623 and 907  $\text{cm}^{-1}$  bands is characteristic of a kaolinite. The presence of Si-O-Si, Si-O-Fe, Al-O-H bands at 1002.14, 1031.09, 457.0 and 914.16  $\text{cm}^{-1}$  respectively is attributed to the quartz.

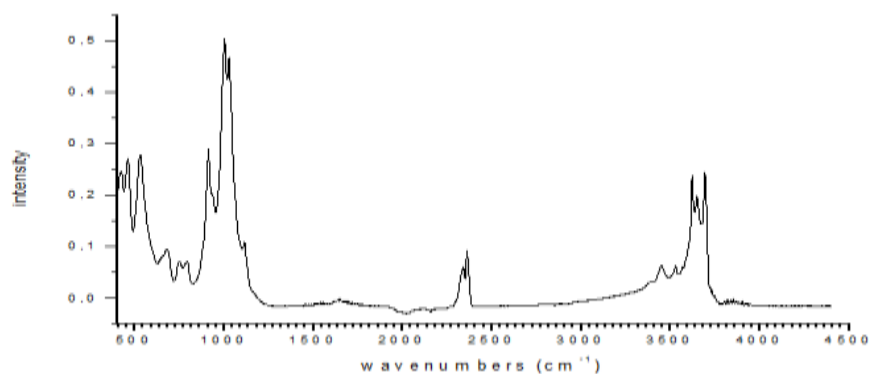


Fig 2: FTIR-ATR Spectra of the clay

The SEM micrograph is represented in the Figure 3a and shows a heterogeneous surface with no particular form. [30, 31]. EDX analysis (fig 3b) was done to confirm the results obtained by XRF. The results obtained by this analysis show that the clay is rich in silica, aluminum and iron.

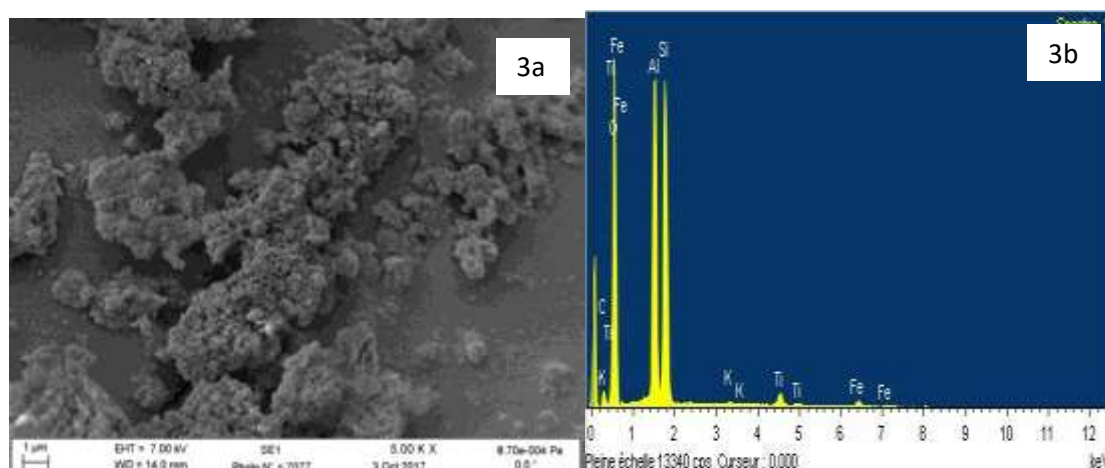


Fig 3: SEM (3a)-EDX (3b) micrograph of Alkibenza clay

The adsorption-desorption isotherm of nitrogen on Alkibenza clay given in Figure 4a shows a hysteresis between 0.74 and 1 P/P<sub>0</sub>. This is indicative of a type IV isotherm, which is characterized by the presence of micropores in the clay material. In fact, the adsorption of nitrogen on Alkibenza clay causes a capillary condensation. That is why the adsorption-desorption curve is not superimposable. The adsorption-desorption process is not a reversible phenomenon in this material. Hence, the distribution of the pores on Alkibenza clay is heterogeneous. According to Figure 4b, the pore volume decreases with an increase in the pore diameter to zero at a pore diameter of 120 nm. This result also confirms that this clay is composed of both micro and meso pores. A measure of diameter by the BJH method gave an average pore diameter of 19.41 nm and a cumulative pore volume of 0.21 cm<sup>3</sup>/g. The BET surface area is 45.62 m<sup>2</sup>/g (Table 2).

Table 2: Surface area and porosity parameters

Parameters	Value
------------	-------

<b>AREA (m<sup>2</sup>/g)</b>	
Single Point Surface Area at P/Po 0.20069150	44.3435
<b>BET Surface Area</b>	45.6293
BJH Adsorption Cumulative Pore Surface Area	44.7953
<b>VOLUME ( cm<sup>3</sup>/ g)</b>	
Single Point Total pore volume less than 156.3257 nm diameter at P/Po 0.98746794	0.221609
BJH Adsorption Cumulative Pore Volume between 1.7 and 300 nm diameter	0.217477
<b>PORE SIZE (nm)</b>	
Average pore diameter ( 4 v/A by BET)	19.4269
BJH Adsorption Average Pore Diameter ( 4V/A)	19.4196

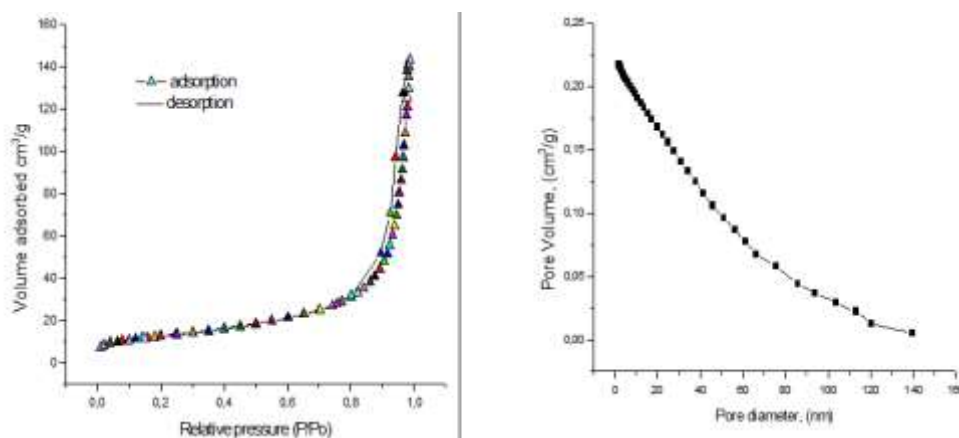


Fig 4a: Sorption of N<sub>2</sub> by the clay and pore volume of the clay Fig 4b: Pore volume distribution of the clay

### Metakaolinite

XRD pattern of metakaolinite illustrated in the fig 5 below shows that some kaolinite's peaks have completely disappeared. These peaks are located at the two theta 12.43 and 18.37. Bands ranging from 2 theta 19.98 to 26 and 35 to 60 have almost disappeared giving room to peaks of low intensity but clearly visible. The disappearance of peaks shows that the thermal activation of kaolinite has expelled some impurities existing in the material [32]. The presence of kaolinite peaks shows that the crystal lattice of kaolinite has not undergone much modification. The new material obtained has an almost amorphous structure

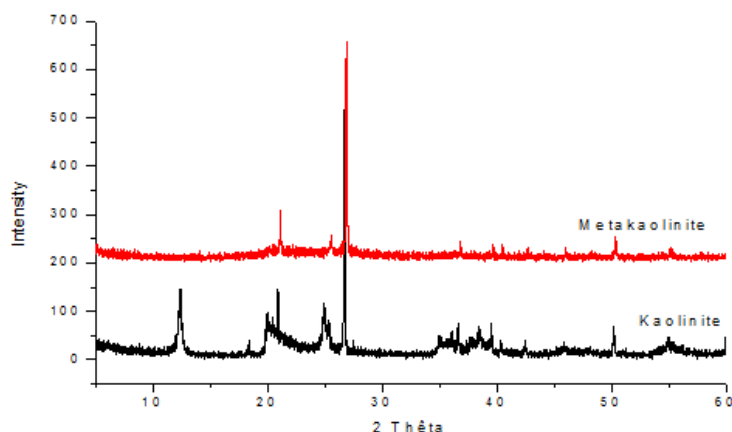


Fig 5 : XRD pattern of metakaolinite compared to that of kaolinite.

The chemical composition of the metakaolin shown in the table 3 below shows some differences in comparison with kaolinite. Proportions of silica and aluminum existing in metakaolinite are slightly higher than those of kaolinite. On the contrary, other elements such as titanium, iron and potassium have small quantities [33]. The analysis shows that the first material (kaolinite) contained impurities. Thermal activation has therefore enriched our precursor in silica and aluminum.

Table 3: Chemical composition of kaolinite and metakaolinite

	Si	Al	Ti	Fe	K	S	P	Ca	Zr	Cr	Cu	Ni	Nb	Ga	Zn	Si/ Al
Kaolinite	49.89	35.40	6.08	5.17	1.18	<1	<1	<1	<1	<1	<1	<1	<1	<1	<1	1.41
	1	1	5	6	3											1
Metakaolinite	49.99	37.54	5.69	4.63	1.13	<1	<1	<1	<1	<1	<1	<1	<1	<1	<1	1.33
	5	6	2	8	2											1

The analysis of the FTIR-ATR spectra of the metakaolinite presented in fig 6 shows peaks at 2364.4, 1056.8, 788.8 and 455.15  $\text{cm}^{-1}$ . Those peaks represent respectively, Si-O-Si vibration (456.8 and 455.15  $\text{cm}^{-1}$ ) and Si-O-Al. The peaks between 3331.16 and 3787.59  $\text{cm}^{-1}$  which are characteristics of the presence of hydroxyl groups have totally disappeared even the peaks at 914.16  $\text{cm}^{-1}$ . All the peaks which were the indication of the presence of the hydroxyl groups have completely disappeared. This result shows that the thermal activation of the clay has reduced its impurities and some hydroxyl groups [34].

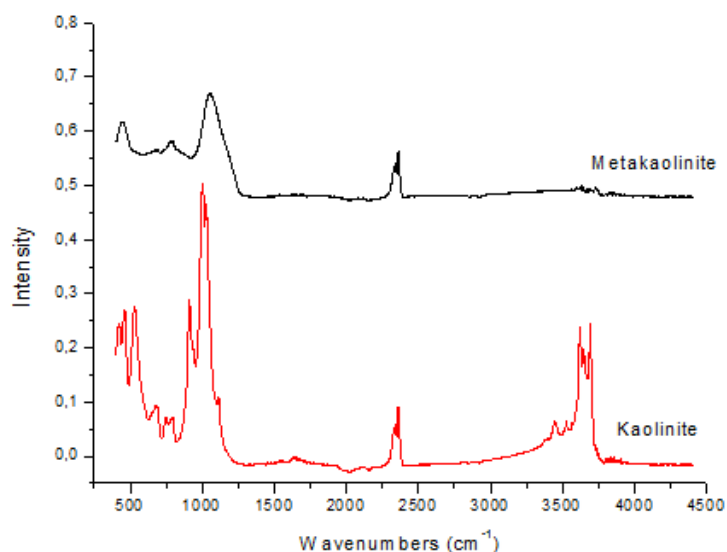


Fig 6: FTIR-ATR spectral of kaolinite and metakaolinite

The analysis of the isotherm of the adsorption of N<sub>2</sub> (Fig 7) on this material shows that the surface of this clay is constituted of meso and micro pores. The pore volume is 0.237 cm<sup>3</sup>/g and the surface area is 45.62 cm<sup>2</sup>/g and the porous diameter are 22.10 nm.

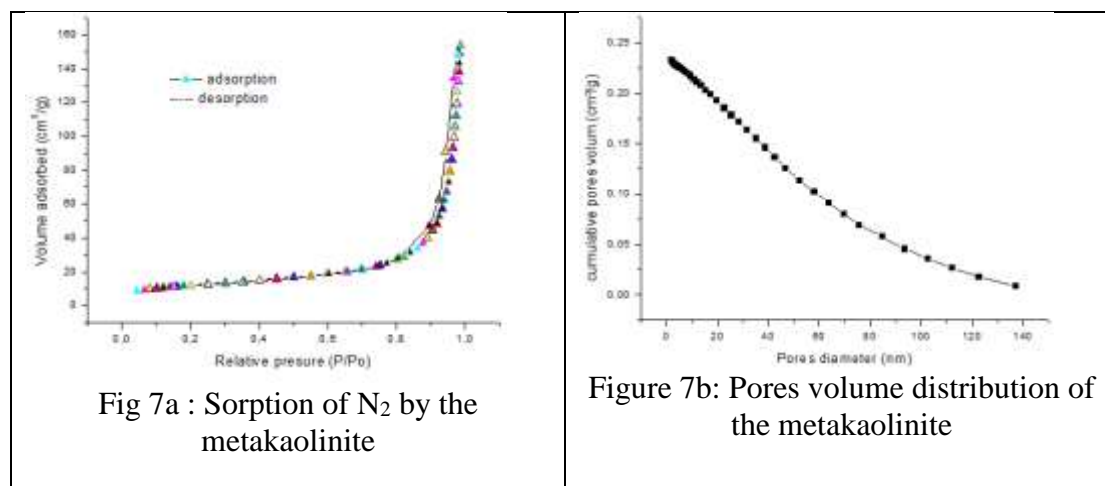
Fig 7a : Sorption of N<sub>2</sub> by the metakaolinite

Figure 7b: Pores volume distribution of the metakaolinite

### Dealuminated Metakaolinite

The XRD spectra's analysis in the figure 8 shows that they have the same crystalline phases. This indicates that the treatment of metakaolin with sulfuric acid did not alter the crystalline phases of our precursor. The dealuminated metakolin obtained in this way still contains silanol and aluminol bonds in its matrix [35]. The analysis of the chemical composition of the dealuminated metakaolinite present in table 5 below shows that this material is richer in silica than in aluminum. Similarly, a comparative analysis of the chemical composition of metakaolin and dealuminated metakaolin shows discrepancies. The proportion of silicon increased from 49.995 in metakaolin to 78.614% in de-aluminated metakaolinite. There is also a decrease in the proportion of aluminum in the de-aluminated metakaolin. The Si / Al ratio in metakaolin is 1.33 and 10.03 in the dealuminated metakaolin (table 4), this result is due to the sulfuric acid's

action on metakaolinite. This indicates that the dealuminated metakaolinite produced can be used for the synthesis of the zeolites Y, because the synthesis of Y-type zeolites requires a precursor very rich in silica.

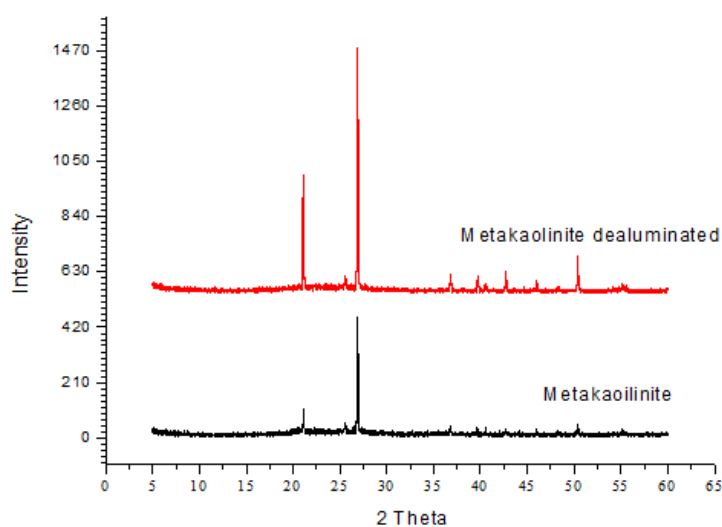


Figure 8: XRD pattern of metakaolinite and metakaolinite dealuminated

Table 4: Chemical composition of METDEA compared to that of Metakaolinite

The table 5 shows the characteristics of the porosity and the surface area of the clay, the metaclay and the metaclay dealuminated.

Chemical element	Chemical composition (%)	
	Metakaolinite	METDEA
Si	49.995	78.614
Al	37.546	7.838
Ti	5.692	9.909
Fe	4.638	1.694
K	1.132	0.331
S	<1	<1
P	<1	<1
Ca	<1	<1
Zr	<1	<1
Cr	<1	<1
Ni	<1	<1
Nb	<1	<1
Ga	<1	<1
Zn	<1	<1
Si/Al	1.33	10.03

Table 5: Surface parameters and porosity of kaolin, metakaolin and metakaon dealuminated

Parameters	Kaolinite	Metakaolini te	METDEA
<b>AREA (m<sup>2</sup>/g)</b>			
Single point Surface Area at P/Po 0.20069150	44.3435	41.6474	123.693
<b>BET Surface Area</b>	45.6293	43.0282	124.551
BJH Adsorption Cumulative Surface Area of pores	44.7953	39.1170	79.37
<b>VOLUME ( Cm<sup>3</sup>/ g)</b>			
Single point Total pore volume of pores less than 156.3257 nm Diameter at P/Po 0.98746794	0.221609	0.237812	79.37
BJH Adsorption Cumulative Pore Volume of pores between 1.7 and 300 nm Diameter	0.217477	0.233150	0.24
<b>PORE SIZE (nm)</b>			
Average pore Diameter ( 4 v/A by BET)	19.4269	22.1076	8.39
BJH Adsorption Average Pore Diameter ( 4V/A)	19.4196	23.8413	13.32

### Zeolite Y

The XRD pattern of the zeolite synthesized is presented in the fig 9 below. According to the data base of the International Zeolite Association, (AIZ, 2017), a zeolite Y is expressed by the presence of the crystalline phases at  $2\theta$  6.18, 10.08, 15.58 and 18.58. These peaks are observed in the zeolite synthesized at  $2\theta$  6.26, 10.17, 11.93, 15.63, 18.68, 23.59 and 31.19 and it fits well with standard zeolite. The small differences observed are attributed to the presence of impurities such as  $Fe^{2+}$ ,  $Ti^{2+}$  and  $Ca^{2+}$  in the Akilbenza clay[36]. Similar results were also obtained for Zeolite Y from metakaolin and metakaolin residus in Brazil and from Elefun kaolinite clay in Nigeria [37, 38]

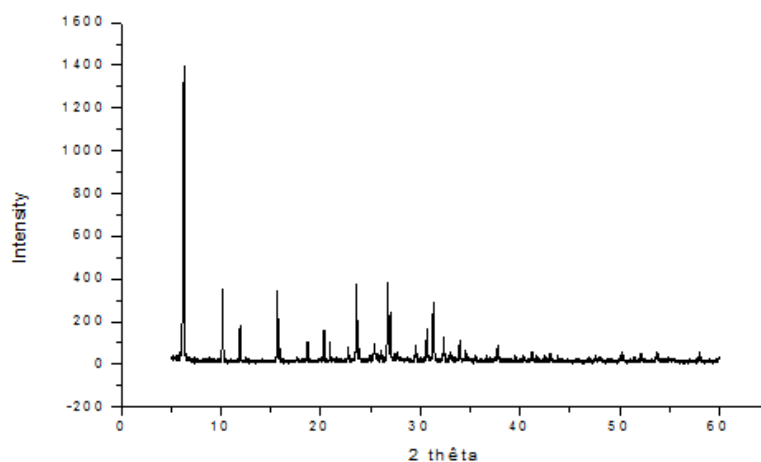


Fig 9: XRD spectral of the zeolite Y synthesized from Akilbenza clay.

The chemical composition of the Y-type zeolite obtained was determined for the purpose of identifying chemical elements assembled in its crystalline mesh. However it should be noted that a Y-type zeolite has aluminum and silica as its main chemical elements, and the Si/Al ratio is between 2 and 5 [3]. The results of the chemical composition's analysis of the zeolite obtained are shown in the table 6 below. The synthesized Y- type zeolite is rich in silica (54.67%) and aluminum (22.12%) which are considered as main elements. Other elements such as titanium and iron are minor elements and the proportion is low. Potassium, zirconium, sodium, manganese, calcium are in trace form. The Si/Al ratio of the zeolite is close to 2.47. Therefore the result obtained is in line with the chemical composition of a Y - type zeolite [14, 39].

Table 6: Chemical composition of zeolite Y

N°	Chemical element	Chemical composition (%)
1	Si	54.67
2	Al	22.12
3	Ti	15.76
4	Fe	4.32
5	K	0.87
6	Zr	0.77
7	Na	0.88
8	Ca	0.49
9	Y	0.02
10	Nb	0.06
11	los	0.04
<b>12</b>	<b>Si/Al</b>	<b>2.47</b>

The FTIR-ATR spectral of the zeolite obtained is presented in the fig 10. It shows the peaks at the wavelengths of 464.80, 798, 707.81, 970.1, 1652.83, 2370.70 and 3432  $\text{cm}^{-1}$ . They represent respectively the stretching of Si-O-Al (464.80 and 707.81  $\text{cm}^{-1}$ ), Si-O (970.1  $\text{cm}^{-1}$ ), Si-OH and Al-OH (2370.29 and 3432  $\text{cm}^{-1}$ ). According to other studies, the peaks between 400 and 1600  $\text{cm}^{-1}$  of this spectra represent the one of a zeolite Y [14, 40, 41]. The presence of the functional groups silanol and aluminol are due to the adsorption of water at the surface of the zeolite.

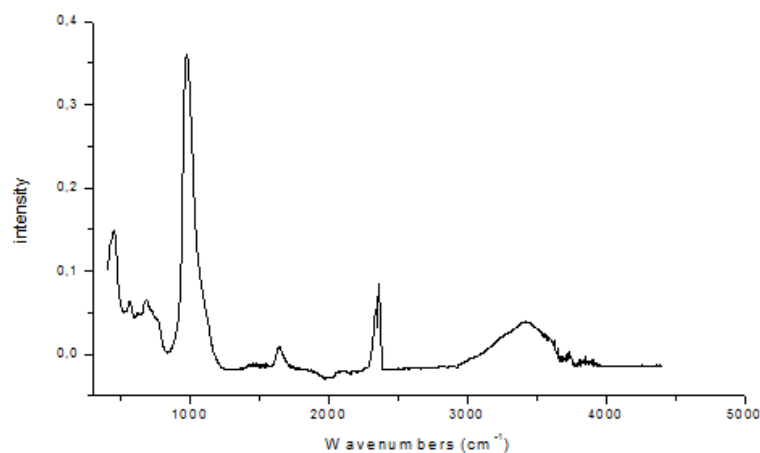


Fig 10 : ATR spectral of zeolite Y from Akilbenza clay

The analysis of the SEM images of this zeolite (Fig 11a) shows a clear octahedral structure which is formed. The analysis of the EDX spectral of this material (Fig 11b) at two areas shows that it is rich in silica and aluminum[41]. The intensity of the silica is higher than the one of alumina. This result confirms the chemical composition of this material obtained from XRF and SEM analysis.

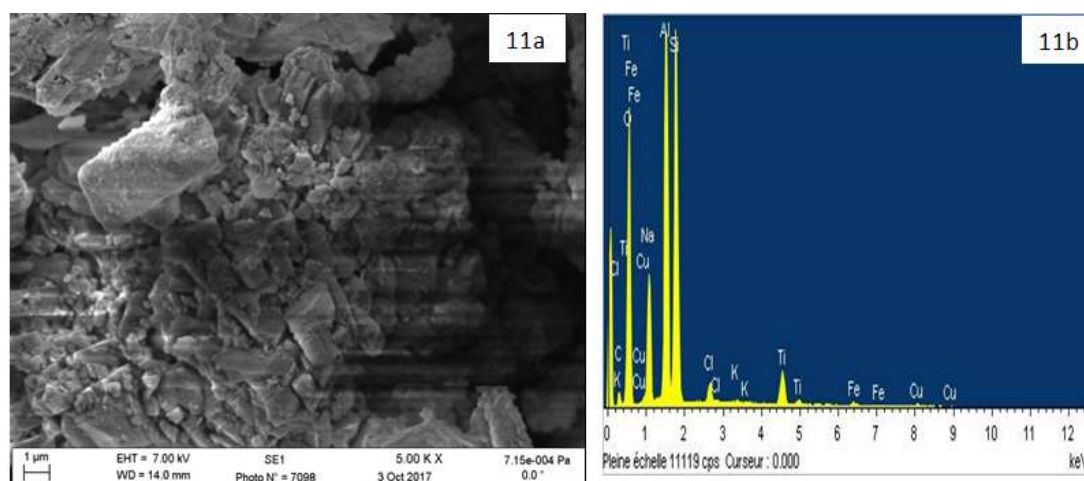


Fig 11: SEM Image (11a) and EDX (11b) spectral of zeolithe Y from Akilbenza clay

The adsorption-desorption isotherm of  $N_2$  on the synthesized zeolite is shown in Fig 12. This isotherm can be divided into three zones. The area between 0 and 0.1  $P/P_0$  has a slight concavity that reflects the formation of a single layer of nitrogen on the zeolite's surface. The result indicates that the adsorption of nitrogen at the surface of the material progressively build up to constitute a monolayer and thus covering the entire external surface of the pores of the zeolite. Zone 2 which lies between 0.1 and 0.9 of  $P/P_0$  is linear and reflects the adsorption of nitrogen on this material on the initial monolayer. Zone 3 which ranges from 0.9 to 1  $P/P_0$  indicates the presence of nitrogen in the pores of the zeolite. The micro-capillary nitrogen thus constitutes a continuous phase. The desorption curve has the same shape like the one of adsorption. However, hysteresis is observed between 1 and 0.5  $P/P_0$ . This shows that the capillary condensation of nitrogen molecules in the pores of the zeolite is not reversible. This is an evidence that the zeolite synthesized has mesopores.

Fig 13 shows the distribution of pore volume as a function of its diameters. From the curve, it should be noted that the pore volume decreases with increase in diameter thereof. This figure has two parts, one between 0 and 5 nm (pore diameter) where the pore volume is high and another part between 5 and 115 nm where the pore volume tends to zero. This result shows that the synthesized zeolite is rich in micro and meso pores. Macropores are not existing within this crystalline structure. Moreover, according to fig 13, the cumulative pore volume decreases with increase in pore diameter until it is annulled around 150 nm. This curve has a high density of cumulative volume between 0 and 10 nm. Also, it shows the strong presence of micropores in the zeolite. Therefore, the zeolite contains more micropores than mesopores. The measurement of the average pore diameter by BJH gave 10.2074 nm and the cumulative

pore volume is  $0.0525 \text{ cm}^3$  (table 7). The result confirms that obtained by the adsorption isotherm and SEM.

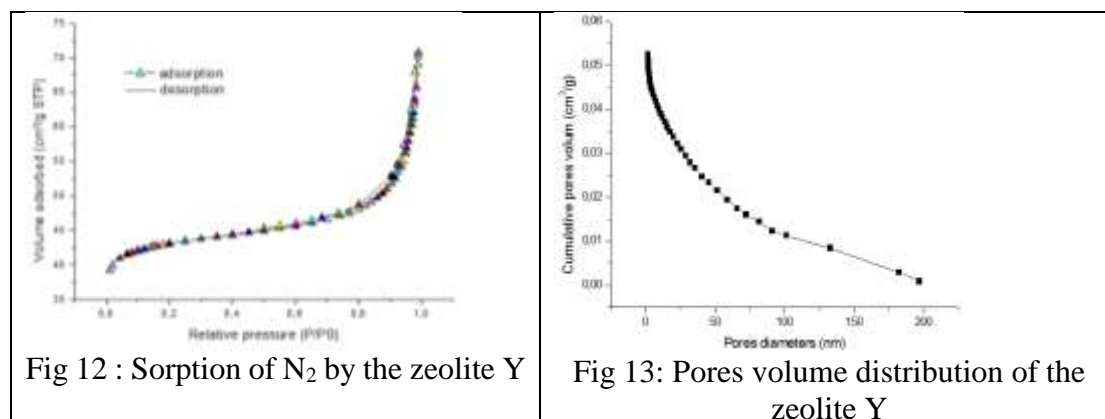


Fig 13: Pores volume distribution of the zeolite Y

Parameters	Value
<b>AREA (m<sup>2</sup>/g)</b>	
Single point Surface Area at P/P <sub>0</sub> 0.20069150	149.88
<b>BET Surface Area</b>	16
	146.74
	64
BJH Adsorption Cumulative Surface Area of pores	20.584
	5
<b>VOLUME ( cm<sup>3</sup>/ g)</b>	
Single point Total pore volume of pores less than 156.3257 nm Diameter at P/P <sub>0</sub> 0.98746794	0.1095
	40
BJH Adsorption Cumulative Pore Volume of pores between 1.7 and 300 nm Diameter	0.0525
	29
<b>PORE SIZE (nm)</b>	
Average pore Diameter ( 4 v/A by BET)	2.9858
BJH Adsorption Average Pore Diameter ( 4V/A)	10.207
	4

### Influence of the crystallization time on the synthesis of the zeolite Y

The XRD pattern of the samples of zeolite Y obtained during the crystallization times from 1 to 4 days of synthesis are presented in the fig 14 below. According to this figure, no peaks showing the synthesis of zeolite are visible during the first day of crystallization. This indicates that new linkages between silica and alumina groups are not yet well established. On the second day, new peaks appear, the most intense are at  $2\theta = 6.16; 10.15; 23.56$  and  $31.23$ . They indicate the initialization of a new crystal formation. All peaks obtained on the second day reappear on the third day with a higher intensity and tend to stabilize on the fourth day. Most intense peaks obtained on the fourth day are at  $2\theta = 6.26, 10.17, 11.93, 15.63, 18.68, 23.59$  and  $31.29$ . All peaks thus obtained from the second to the fourth day of crystallization compare well with

those of a Y - type zeolite [42, 43]. From these results, we can mention that a Y - type zeolite' synthesis using this clay material requires four days of crystallization and that increase in crystallization time increases the growth of the crystal. These results are in agreement with with some works in literature [44, 45]. However, they do not agree with a recent study carried out in 2018 which reported the synthesis of zeolite Y from kaolin Bangka within 30h [15]. The difference between these two studies may be attributed to the degree of cristalinity in Akilbenza kaolin and the quality of metakaolinization carried out.

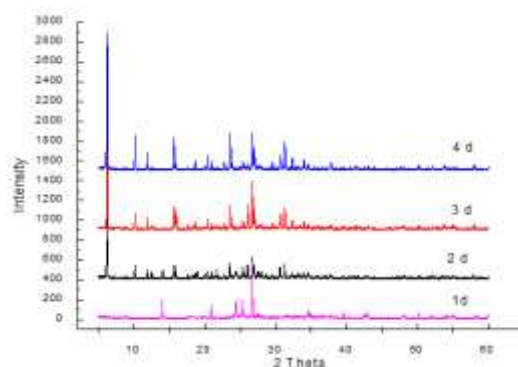


Fig 14: XRD pattern of zeolite Y from Akilbenza clay during 1, 2, 3 and 4 day of crystallization time

Synthesized zeolite samples' FTIR-ATR spectra during 1, 2, 3 and 4 days are shown in figure 15 below. From them, we notice the presence of peaks that range from 400 to 1200  $\text{cm}^{-1}$ . They represent Si-O-Si ( $970.099 \text{ cm}^{-1}$ ) and Si-O-Al ( $464, 798, 707.805 \text{ cm}^{-1}$ ) functions. those peaks indicate the Y zeolite's formation [46]. The result shows that during the first day of crystallization, basic chemical bonds on which the growth of the crystal will be done are formed. That is why the same functional groups are present in the other FTIR-ATR spectra during the other days of crystallization. The FTIR-ATR spectrum's interpretation of zeolites synthesized during 1, 2, 3 and 4 days of crystallization shows that favourable chemical functions for crystal growth are stable as from the second day of crystallization as specified in figure 15 below.

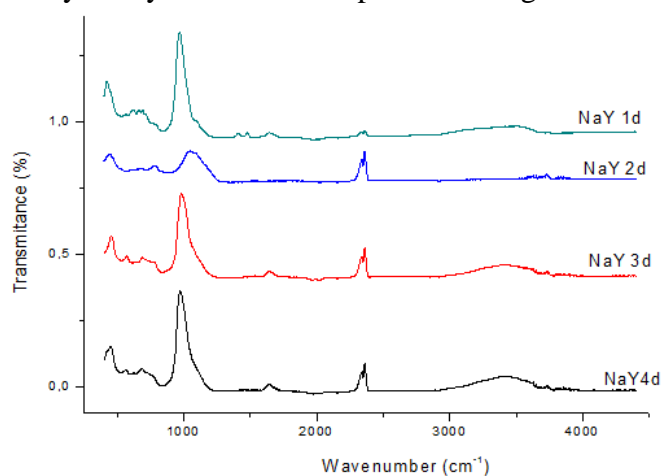


Fig 15 : FTIR-ATR spectra of zeolite Y from Akilbenza clay during 1, 2, 3 and 4 day of crystallization time

The chemical composition of each product obtained for crystallization times of 1, 2, 3 and 4 days together with the XRF analysis are shown in the table 8. The elements present with high proportions are silica and alumina. Titanium and iron atoms are there in low fractions. The proportion of other elements such as potassium, zirconium, sodium, calcium, yttrium, and niobium are lowest. The ratio of Si/Al obtained from those materials are 1.95 (day1); 2.78 (day2), 2.81 (day3) and 2.47 (day4). This result can be explained by the fact that, during the first day, the crystallization time which was supposed to allow the stabilization of chemical bonds is not yet reached. It is for this reason that a value of the Si/Al ratio which is not close to that of a Y-type zeolite was obtained, but however from the second day until the fourth day of crystallization, this value of the ratio Si/Al is similar to that of zeolite Y [47]. This result shows that, the zeolite Y has been effectively synthesized and from the second day of crystallization, the zeolite obtained has a trend to be stabilized and the crystal is more rigid. This result is in agreement with the one obtained from the XRD analysis of these materials. This shows that the crystallization time has an effect on the chemical composition of the zeolite synthesised.

Table 8 : Chemical composition of zeolite obtained on 1, 2, 3 and 4 days of crystallization

N°	Chemical element	NaY 1d	NaY 2d	NaY 3d	NaY 4d
1	Si	42.11	59.68	58.99	54.67
2	Al	21.55	21.43	20.97	22.12
3	Ti	28.89	13.19	13.71	15.76
4	Fe	5.26	3.54	3.13	4.32
5	K	0.24	0.63	0.75	0.87
6	Zr	1.23	0.63	0.70	0.77
7	Na	0.18	0.23	0.80	0.88
8	Ca	0.30	0.60	0.50	0.49
9	Y	0.03	0.02	0.02	0.02
10	Nb	0.05	0.05	0.05	0.06
11	los	0.16	0.63	3.38	0.04
<b>12</b>	<b>Si/Al</b>	<b>1.95</b>	<b>2.78</b>	<b>2.81</b>	<b>2.47</b>

The SEM images of the zeolite obtained during the crystallization times of 1, 2, 3 and 4 day are presented in the fig16. This result shows that, during the first day, the zeolite obtained does not show a particular form. But from the second day, there is an appearance of an octahedral form. This is very precise with increasing crystallization time. On the fourth day, the octahedral form obtained is well established. This shows that crystallization time has an effect on the morphology of the zeolite. With an increase of the crystallization time, the crystalline form is well established and indicates the stability of the crystalline form.

The observation of the surface of those materials at any given crystallization time shows that, during the first day, the surface of this material is not porous. But from the second day of crystallization, there is an appearance of pores with different diameters. The sizes of these pores decrease with an increase in the crystallization time as it is shown in the image obtained on the third day. That is why during the fourth day, these pore sizes

further grow small. This is explained by the fact that, the growth of the crystal occupies progressively wide spaces within the crystalline structure with the crystalline time.

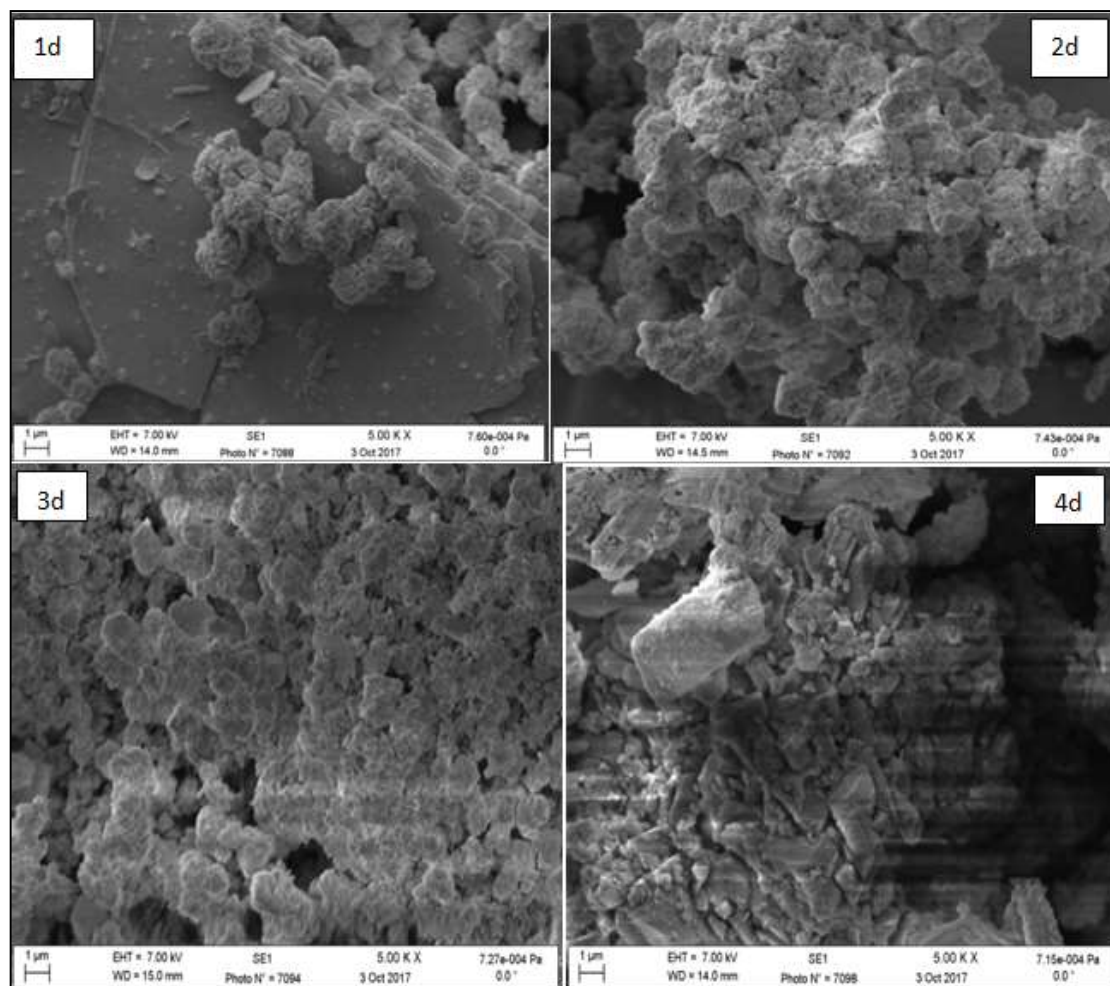


Figure 16: SEM Images of zeolite Y from Akilbenza clay during 1, 2, 3 and 4 day of crystallization time.

The analysis of the EDX spectral of the zeolite obtained during 1, 2, 3 and 4 days of the crystallization times (fig 17) shows that all these materials are mainly rich in silica and alumina. The chemical elements such as iron and titanium have lower peak intensities. This result is in conformity with the XRF of these materials. According to the second spectral, the intensity of the silica atom is higher than that of the alumina atom. From the second day, this intensity of the silica atom looks double compared to that of alumina. The same observation is made for the third and fourth day. This result shows that from the second day of crystallization, if the ratio Si/Al is taken into consideration, the product obtained is zeolite Y [7]. This result confirms the one obtained from the XRF of those materials.

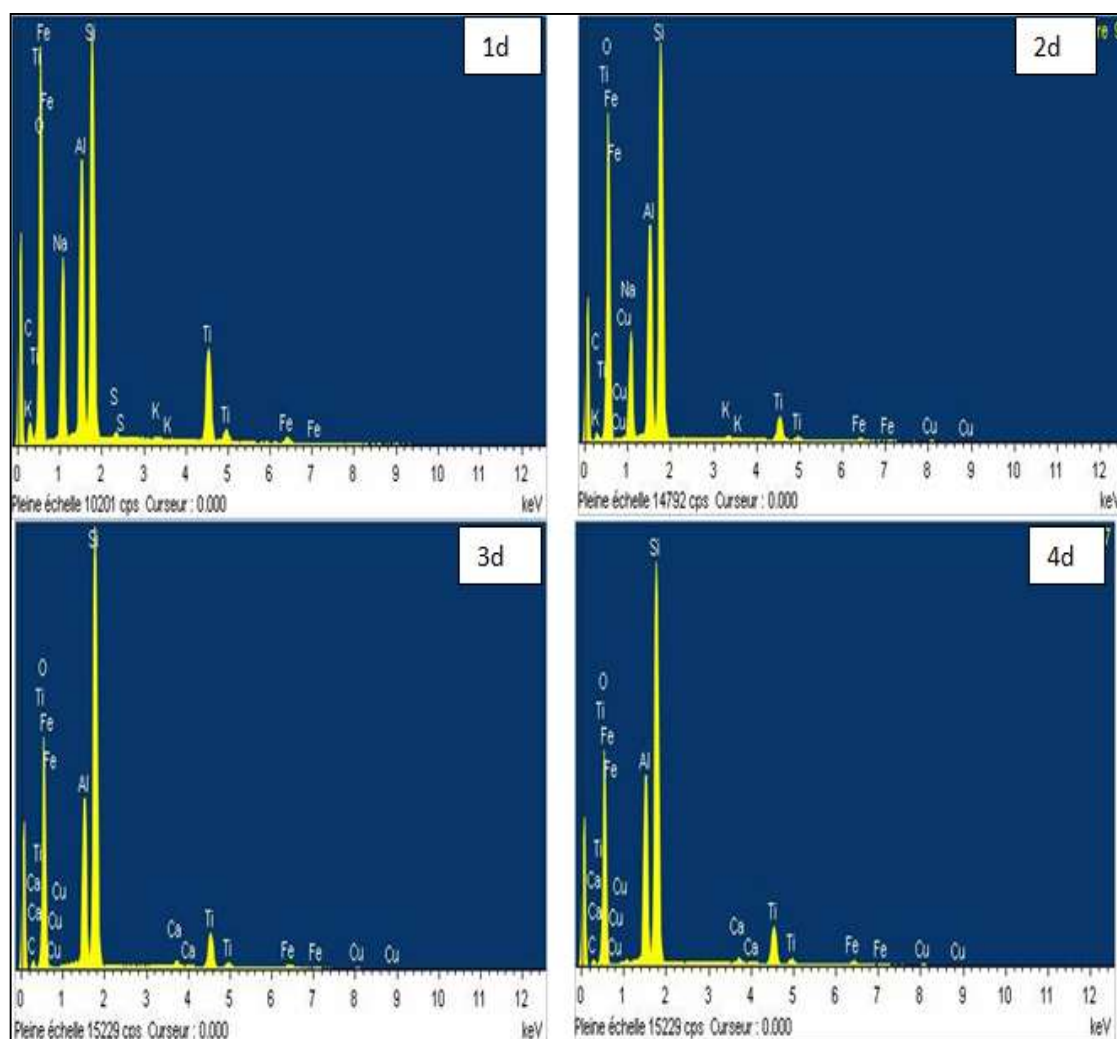


Fig 17: EDX pattern of zeolite Y from Akilbenza clay during 1, 2, 3 and 4 day of crystallization time

## CONCLUSION

At the end of this work, it can be ascertained that a pure zeolite was synthesized from the clay of Akilbenza. A zeolite Y was obtained at a crystallization time of 4 days, a crystallization temperature of 110°C and at the ageing time of 24 h. The study of the influence of crystallization time shows that at least two days of crystallization is required for this synthesis and the growth of the crystal increases with crystallization time. This work shows how the clay from Akilbenza can be used as a reference for the synthesis of the zeolite Y.

## REFERENCES

- [1] X. Querol, F. Plana, A. Alastuey, A. López-Soler, Synthesis of Na-zeolites from fly ash, *Fuel*, 76 (1997) 793-799.
- [2] A. Chaisena, K. Rangriwatananon, Synthesis of sodium zeolites from natural and modified diatomite, *Materials letters*, 59 (2005) 1474-1479.

- [3] D. Georgiev, B. Bogdanov, K. Angelova, I. Markovska, Y. Hristov, Synthetic zeolites–Structure, classification, current trends in zeolite synthesis, in: Economics and Society Development on the Base of Knowledge: International Scientific Conference, 2009.
- [4] T.T. Walek, F. Saito, Q. Zhang, The effect of low solid/liquid ratio on hydrothermal synthesis of zeolites from fly ash, *Fuel*, 87 (2008) 3194-3199.
- [5] H. Mimura, K. Yokota, K. Akiba, Y. Onodera, Alkali hydrothermal synthesis of zeolites from coal fly ash and their uptake properties of cesium ion, *Journal of nuclear Science and Technology*, 38 (2001) 766-772.
- [6] J. Cejka, A. Corma, S. Zones, *Zeolites and catalysis: synthesis, reactions and applications*, John Wiley & Sons, 2010.
- [7] B.A. Holmberg, H. Wang, Y. Yan, High silica zeolite Y nanocrystals by dealumination and direct synthesis, *Microporous and Mesoporous Materials*, 74 (2004) 189-198.
- [8] A. Arafat, J. Jansen, A. Ebaid, H. Van Bekkum, Microwave preparation of zeolite Y and ZSM-5, *Zeolites*, 13 (1993) 162-165.
- [9] Y. Wang, F. Lin, W. Pang, Ion exchange of ammonium in natural and synthesized zeolites, *Journal of Hazardous Materials*, 160 (2008) 371-375.
- [10] J. Zhu, Y. Cui, Y. Wang, F. Wei, Direct synthesis of hierarchical zeolite from a natural layered material, *Chemical Communications*, (2009) 3282-3284.
- [11] G.E. Christidis, H. Papantoni, Synthesis of FAU type zeolite Y from natural raw materials: hydrothermal SiO<sub>2</sub>-Sinter and Perlite glass, *The open mineralogy journal*, 2 (2008).
- [12] E. Johnson, S.E. Arshad, Hydrothermally synthesized zeolites based on kaolinite: a review, *Applied Clay Science*, 97 (2014) 215-221.
- [13] R.E. Grim, *Applied clay mineralogy*, (1962).
- [14] A. Kovo, O. Hernandez, S. Holmes, Synthesis and characterization of zeolite Y and ZSM-5 from Nigerian Ahoko Kaolin using a novel, lower temperature, metakaolinitization technique, *Journal of Materials Chemistry*, 19 (2009) 6207-6212.
- [15] Y. Bai, W. Wu, X. Bian, Dynamic synthesis route of zeolite Y with kaolin to improve yield, *Green Processing and Synthesis*, 7 (2018) 23-29.
- [16] G. Sun, Y. Liu, J. Yang, J. Wang, Seeded synthesis of small polycrystalline NaY zeolite membrane using zeolite structure-directing agent and its pervaporation performance, *Journal of Porous Materials*, 18 (2011) 465-473.
- [17] M.M. Htay, M.M. Oo, Preparation of Zeolite Y catalyst for petroleum cracking, *World Academy of Science, Engineering and Technology*, 48 (2008) 114-120.
- [18] M. Hajjaji, S. Kacim, A. Alami, A. El Bouadili, M. El Mountassir, Chemical and mineralogical characterization of a clay taken from the Moroccan Meseta and a study of the interaction between its fine fraction and methylene blue, *applied clay science*, 20 (2001) 1-12.
- [19] E. Horváth, R.L. Frost, É. Makó, J. Kristóf, T. Cseh, Thermal treatment of mechanochemically activated kaolinite, *Thermochimica Acta*, 404 (2003) 227-234.
- [20] M.-q. Jiang, Q.-p. Wang, X.-y. Jin, Z.-l. Chen, Removal of Pb (II) from aqueous solution using modified and unmodified kaolinite clay, *Journal of Hazardous Materials*, 170 (2009) 332-339.
- [21] M.-q. Jiang, X.-y. Jin, X.-Q. Lu, Z.-l. Chen, Adsorption of Pb (II), Cd (II), Ni (II) and Cu (II) onto natural kaolinite clay, *Desalination*, 252 (2010) 33-39.

- [22] A. Sari, M. Tuzen, D. Citak, M. Soylak, Equilibrium, kinetic and thermodynamic studies of adsorption of Pb (II) from aqueous solution onto Turkish kaolinite clay, *Journal of Hazardous Materials*, 149 (2007) 283-291.
- [23] A.K. Panda, B.G. Mishra, D.K. Mishra, R.K. Singh, Effect of sulphuric acid treatment on the physico-chemical characteristics of kaolin clay, *Colloids and Surfaces A: Physicochemical and Engineering Aspects*, 363 (2010) 98-104.
- [24] C. Quintelas, Z. Rocha, B. Silva, B. Fonseca, H. Figueiredo, T. Tavares, Removal of Cd (II), Cr (VI), Fe (III) and Ni (II) from aqueous solutions by an E. coli biofilm supported on kaolin, *Chemical Engineering Journal*, 149 (2009) 319-324.
- [25] Y.-h. Hu, X.-w. Liu, Chemical composition and surface property of kaolins, *Minerals Engineering*, 16 (2003) 1279-1284.
- [26] R.L. Frost, A.M. Vassallo, The dehydroxylation of the kaolinite clay minerals using infrared emission spectroscopy, *Clays and Clay minerals*, 44 (1996) 635-651.
- [27] B.J. Saikia, G. Parthasarathy, Fourier transform infrared spectroscopic characterization of kaolinite from Assam and Meghalaya, Northeastern India, *Journal of Modern Physics*, 1 (2010) 206.
- [28] P.S. Nayak, B. Singh, Instrumental characterization of clay by XRF, XRD and FTIR, *Bulletin of Materials Science*, 30 (2007) 235-238.
- [29] M. Eloussaief, N. Kallel, A. Yaacoubi, M. Benzina, Mineralogical identification, spectroscopic characterization, and potential environmental use of natural clay materials on chromate removal from aqueous solutions, *Chemical Engineering Journal*, 168 (2011) 1024-1031.
- [30] K. Konan, C. Peyratout, A. Smith, J.-P. Bonnet, S. Rossignol, S. Oyetola, Comparison of surface properties between kaolin and metakaolin in concentrated lime solutions, *Journal of colloid and interface science*, 339 (2009) 103-109.
- [31] T. Cheng, M. Lee, M. Ko, T. Ueng, S. Yang, The heavy metal adsorption characteristics on metakaolin-based geopolymer, *Applied Clay Science*, 56 (2012) 90-96.
- [32] B.R. Ilić, A.A. Mitrović, L.R. Miličić, Thermal treatment of kaolin clay to obtain metakaolin, *Hemijaska industrija*, 64 (2010) 351-356.
- [33] B. Sabir, S. Wild, J. Bai, Metakaolin and calcined clays as pozzolans for concrete: a review, *Cement and concrete composites*, 23 (2001) 441-454.
- [34] M. Murat, Hydration reaction and hardening of calcined clays and related minerals. I. Preliminary investigation on metakaolinite, *Cement and Concrete Research*, 13 (1983) 259-266.
- [35] M. Lenarda, L. Storaro, A. Talon, E. Moretti, P. Riello, Solid acid catalysts from clays: Preparation of mesoporous catalysts by chemical activation of metakaolin under acid conditions, *Journal of colloid and interface science*, 311 (2007) 537-543.
- [36] Y. Krisnandi, I. Parmanti, R. Yunarti, R. Sihombing, I. Saragi, Synthesis and Characterization of Zeolite NaY from kaolin Bangka Belitung with variation of synthesis composition and crystallization time, in: *Journal of Physics: Conference Series*, IOP Publishing, 2018, pp. 012043.
- [37] L.B. Bortolatto, R.A.B. Santa, J.C. Moreira, D.B. Machado, M.A.P. Martins, M.A. Fiori, N.C. Kuhnen, H.G. Riella, Synthesis and characterization of Y zeolites from alternative silicon and aluminium sources, *Microporous and Mesoporous Materials*, 248 (2017) 214-221.

- [38] A. Ayoola, F. Hymore, M. Ojewumi, O.J. Uwoghiren, Effects of Sodium Hydroxide Concentration on Zeolite Y Synthesized from Elefun Kaolinite Clay in Nigeria, *International Journal of Applied Engineering Research*, 13 (2018) 1536-1536.
- [39] Y.K. Krisnandi, I.R. Saragi, R. Sihombing, R. Ekananda, I.P. Sari, B.E. Griffith, J.V. Hanna, Synthesis and Characterization of Crystalline NaY-Zeolite from Belitung Kaolin as Catalyst for n-Hexadecane Cracking, *Crystals*, 9 (2019) 404.
- [40] E. Drag, A. Miecznikowski, F. Abo-Lemon, M. Rutkowski, Synthesis of A, X and Y zeolites from clay minerals, in: *Studies in Surface Science and Catalysis*, Elsevier, 1985, pp. 147-154.
- [41] P. Krongkrachang, P. Thungngern, P. Asawaworarit, N. Hounkamhang, A. Eiad-Ua, Synthesis of Zeolite Y from Kaolin via hydrothermal method, *Materials Today: Proceedings*, 17 (2019) 1431-1436.
- [42] H. Faghihian, N. Godazandeha, Synthesis of nano crystalline zeolite Y from bentonite, *Journal of Porous Materials*, 16 (2009) 331-335.
- [43] M. Htay, M.M. Oo, Preparation of Zeolite Y catalyst for petroleum cracking, *World Academy of Science, Engineering and Technology*, 48 (2008) 114-120.
- [44] X. Zhang, D. Tong, W. Jia, D. Tang, X. Li, R. Yang, Studies on room-temperature synthesis of zeolite NaA, *Materials Research Bulletin*, 52 (2014) 96-102.
- [45] C.R. Melo, H.G. Riella, N.C. Kuhnen, E. Angioletto, A.R. Melo, A.M. Bernardin, M.R. da Rocha, L. da Silva, Synthesis of 4A zeolites from kaolin for obtaining 5A zeolites through ionic exchange for adsorption of arsenic, *Materials Science and Engineering: B*, 177 (2012) 345-349.
- [46] S. Ferchiche, J. Warzywoda, A. Sacco Jr, Direct synthesis of zeolite Y with large particle size, *International Journal of Inorganic Materials*, 3 (2001) 773-780.
- [47] E.I. Basaldella, R. Bonetto, J.C. Tara, Synthesis of NaY zeolite on preformed kaolinite spheres. Evolution of zeolite content and textural properties with the reaction time, *Industrial & engineering chemistry research*, 32 (1993) 751-752.